A Comparative Study of the Gut Microbiota Associated with Immunoglobulin A Nephropathy and Membranous Nephropathy

shiren sun (sunshiren1212@163.com)

Department of Nephrology, Xijing Hospital, the Fourth Military Medical University, Xi,an, Shaanxi, China
https://orcid.org/0000-0002-8691-2101

Ruijuan Dong

Department of Nephrology, Xijing Hospital, the Fourth Military Medical University, Xi,an, Shaanxi, China

Ming Bai

Department of Nephrology, Xijing Hospital, the Fourth Military Medical University, Xi,an, Shaanxi, China

Jin Zhao

Department of Nephrology, Xijing Hospital, the Fourth Military Medical University, Xi'an, Shaanxi, China

Di Wang

Department of Nephrology, Xijing Hospital, the Fourth Military Medical University, Xi'an, Shaanxi, China

Xiaoxuan Ning

Department of Geriatrics, Xijing Hospital, the Fourth Military Medical University, Xi'an, Shaanxi, China

Research

Keywords: Gut microbiota, Immunoglobulin A nephropathy, Membranous nephropathy

Posted Date: February 26th, 2020

DOI: https://doi.org/10.21203/rs.2.24727/v1

Abstract

Background The pathogenesis of immunoglobulin A nephropathy (IgAN) and membranous nephropathy (MN) is characterized by immune dysregulation, which is related to gut dysbiosis. The aim of the study was to compare the gut microbiota of patients with IgAN and MN versus healthy controls. We used 16S rDNA amplicon sequencing to investigate the bacterial communities of 44 patients with kidney biopsy-proven IgAN, 40 patients with kidney biopsy-proven MN, and 30 matched healthy controls (HC). Results The abundance of Escherichia-Shigella and Defluviitaleaceae_incertae_sedis were significantly higher in IgAN than in HC, whereas lower abundances were observed for Roseburia, Lachnospiraceae_ unclassified, Clostridium_sensu_stricto_1, and Fusobacterium . Furthermore, the abundance of Escherichia-Shigella, Peptostreptococcaceae_incertae_sedis , Streptococcus, and Enterobacteriaceae_ unclassified increased, while that of Lachnospira, Lachnospiraceae_ unclassified, Clostridium_sensu_stricto_1, and Veillonella decreased in MN. The abundance of Megasphaera and Bilophila was higher, whereas that of Megamonas, Veillonella, Klebsiella, and Streptococcus was lower in patients with IgAN than in those with MN. Analysis of the correlations showed that in the IgAN group, Prevotella was positively correlated, while Klebsiella , Citrobacter, and Fusobacterium were negatively correlated with the level of serum albumin. Positive correlation also existed between Bilophila and Crescents in the Oxford classification of IgAN. In the MN group, negative correlation was observed between Escherichia-Shigella and proteinuria, Bacteroides and Klebsiella showed positive correlation with the MN stage. Conclusions Patients with IgAN and MN exhibited gut microbial signatures distinct from healthy controls. Our study suggests the potential of gut microbiota as specific biomarker and contributor in the pathogenesis of IgAN and MN.

Background

The gut microbiome, residing at intestinal epithelial barriers, is recognized as an important element that contributes to health and disease[1]. Dysregulation in the interactions between the gut microbial ecosystem and the adjacent mucosal immune system have been identified in Crohn's disease (CD)[2] and ulcerative colitis (UC)[3]. Increasing evidence indicates that gut dysbiosis is associated with other immune-mediated diseases, including systemic lupus erythematous (SLE)[4], ankylosing spondylitis[5] and rheumatoid arthritis(RA)[6], where abnormal immune response affect sites distant from the gut. However, a mechanistic connection between the gut microbiota and extra-intestinal immune-mediated diseases remains unclear.

IgA nephropathy (IgAN), the most prevalent primary glomerulonephritis[7], is characterized by the deposition of IgA1(particularly, galactose-deficient IgA1) in the glomerular mesangium[8]. Galactose-deficient IgA1, supposed to be produced by Peyer patches in the mucosa-associated lymphoid tissue(MALT)[8], is triggered by exposure to commensal or pathogenic bacteria[9] and is involved in the initial step in the pathogenesis of IgAN. A previous study showed that certain new risk loci for IgA nephropathy are associated with the maintenance of the intestinal epithelial barrier and response to mucosal pathogens[10]. The complex crosstalk between the gut and the kidney in IgAN has been

elucidated and the gut-kidney axis has been supposed[11]. Studies have suggested that gut dysbiosis may contribute to the onset and progression of IgAN; however, no clear causal associations have been demonstrated so far.

Membranous nephropathy (MN), the most common cause of adult-onset nephrotic syndrome worldwide, is an immune-mediated glomerular disease[12]. Muscle-type phospholipase A2 receptor (PLA2R)[13] and thrombospondintype-1 domain-containing 7A (THSD7A)[14] were identified as the target antigens. Autoantibodies to both target antigens are predominantly of the IgG4 subclass[15]. Cationic bovine serum albumin, identified as the main antigen in early-childhood membranous nephropathy, may derive from microbiota, intestinal cells and milk formula[16]. Clonal expansion of B cells, promoted by MALT [19], may induce autoantibody production by interacting with genetic polymorphisms[20]. With this background, therefore, we hypothesized that gut dysbiosis is possibly involved in the etiopathogenesis of MN.In this study, we aimed to investigate the association between the gut microbiota and the pathogenesis of IgAN and MN; toward this, we analyzed the bacterial community composition and diversity in patients and healthy controls using 16S ribosomal DNA Miseq sequencing. We report herein substantial differences in the composition of the gut microbiota between patients and healthy controls. Furthermore, we identify taxonomic biomarkers associated with clinical parameters. This study presents a picture of the microbiota in patients with IgAN and MN and offers specific biomarkers that may potentially contribute to the pathogenesis of IgAN and MN.

Methods

Study Population

We enrolled 44 patients with kidney biopsy-proven IgAN and 40 patients with kidney biopsy-proven MN who did not receive corticosteroids and/or immunosuppressive therapies prior to sampling, along with 30 matched healthy controls. All patients with IgAN and MN were recruited between September 2017 and May 2019 from the inpatient department of the Xijing Hospital. Patients with secondary glomerulonephritis, renovascular disease, gastro-intestinal diseases, pregnancy, and other autoimmune disorders were excluded. Healthy controls were enrolled from physical examination center volunteers. None of the individuals had taken antibiotics or probiotics/prebiotics for at least 3 months prior to sample collection. All individuals confirmed that there were no significant differences in meals and other lifestyle-related factors for at least 2 weeks. The demographic data, including gender, age, and body mass index (BMI), clinical features, results of biochemical examination, and biopsy-based pathological manifestations were recorded (Supplemental Table 1).

Collection of Faecal Samples and DNA Extraction

Fresh faecal samples were collected from the recruited individuals in the morning. After collection, the samples were immediately frozen and stored at -80°C prior to analyses. The faecal sample was added to a 2ml screwcap vial containing 1g glass beads (0.1mm BioSpec Products, Inc., USA) and was suspended

in 790µl sterile lysis buffer (4M guanidine thiocyanate; 10% N-lauroylsarcosine; 5% N-lauroyl sarcosine-0.1 M phosphate buffer, pH 8.0). The samples were subjected to bead beating for 10 min at maximum speed prior to incubation at70℃ for 1 h. Microbial DNA was extracted using the E.Z.N.A.®Stool DNA kit (Omega Bio-tek, Inc., GA,USA).

Polymerase Chain Reaction (PCR), Miseq Sequencing and Sequence Data Processing

The V3-V4 hypervariable regions of the 16S rDNA were amplified with primers 341F (5'-CCTACGGGNGGCWGCAG-3') and 805R (5'-GACTACHVGGGTATCTAATCC-3') using an EasyCycler 96 (PCR) system (Analytik Jena Corp., AG, Germany). PCR was conducted using the following program: 3 min of denaturation at 95℃, 21 cycles of 0.5 min at 94℃ (denaturation), 0.5 min for annealing at 58℃, 0.5 min at 72℃, and 5 min at 72℃ for a final extension. PCR was performed in a 20-µl reaction system containing 4µl 5×Fastpfu buffer, 2 µl 2.5 mM deoxynucleotide triphosphates (dNTPs), 0.8 µl of each primer (5 µM), 0.4 µl TransStart Fastpfu DNA polymerase (TransGen Biotech, Beijing, China), and 10 ng template DNA. The PCR products were detected on a 2% agarose gel, and the band was extracted and purified using the AxyPrepDNA gel (Axygen, CA, USA) and PCR clean-up system. The purified PCR products were mixed. Sequencing was performed on an Illumina MiSeq platform according to the standard protocols of the Shanghai Mobio Biomedical Technology Co. Ltd., China. The raw read data of all the samples have been deposited in the European Bioinformatics Institute European Nucleotide Archive database under the accession number: PRJNA574226.

Bioinformatics and Statistical analysis

The raw data were processed using FLASH with the following criteria: (1) longer than 200bp; (2) less than two mismatches of primers; (3) no ambiguous bases; (4) longer than 10 bp overlap in sequences that were merged according to their sequence.

Operational taxonomic units (OTUs) were clustered with 97% similarity cutoff using UPARSE(version 7.1 http://drive5.com/uparse/) with the following steps: (1) non-repeating sequences were extracted from the optimized sequences; (2) singletons of non-repeating sequences were removed; (3) OTUs were picked at 97% similarity cutoff; (4) OTU composition was created. The Ribosomal Database Project (RDP) Classifier algorithm(http://rdp.cme.msu.edu) was applied to analyze the taxonomy of each 16S rDNA sequence using the SILVA database(http://www.arb-silva.de). After filtering, we generated an average of 49,775 reads for each sample.

Species accumulation curve was plotted to evaluate the sufficiency of sample size and estimate bacterial richness. α-Diversity was determined using OTU analysis and presented using ACE index, chao index, Shannon index, and Simpson index, which were analyzed using the implemented method in the R package ‘vegan’. The details are showed in the Supplemental Table 2. Bacterial taxonomic comparison at the phylum and genus levels was tested between two groups using Wilcoxon rank sum test. β-Diversity was measured using unweighted UniFrac distances. Principal coordinate analysis (PCoA) was performed to display the space between samples. Linear discriminant analysis (LDA) effect size (LEfSe) was used to identify the characteristic microbiota and explain the differences between the patients and healthy

controls. Different characterizations were performed with an LDA cut-off of 2.0. For correlation analysis, Spearman's rank test was performed. The two-tailed t-test was used to evaluate continuous variables and the Chi-square test was used to compare categorical variables between the two groups. Statistical analyses were performed using SPSS V.20.0 for Windows (SPSS, Chicago, Illinois, USA).*P* values were considered significant at $P<0.05$.

Results

Clinical Characteristics of all Participants

We recruited 44 patients with IgAN, 40 patients with MN, and 30 healthy controls. All the patients were newly diagnosed with the conditions using kidney biopsy. The clinical characteristics of the participants are shown in Table 1. Age, gender, and BMI were matched between the patients and healthy controls. As expected, serum creatinine level was higher in patients with IgAN than in healthy controls, while the serum levels of total protein and albumin were significantly lower in patients with MN than in healthy controls (Table 1). The median proteinuria of patients with IgAN was 776mg/24h, whereas that of patients with MN was 3,623mg/24h. About 72.5% of patients with MN presented with positivity of serum anti-PLA2R antibodies. According to the Oxford classification of IgAN, there was modest glomerulonephritis with mild tubulointerstitial injury. Approximately 35(87.5%) patients presented with stage □ MN (Table 2).

Richness and Diversity of the Gut Microbiota

In total, 6,337,125 usable raw reads were obtained from 114 stool samples. After quality filtering and assembly of overlapping paired-end reads, 5,674,350 high-quality reads were generated and 698 operational taxonomic units (OTUs) were obtained based on a 97% homology cutoff. The average number of sequences per sample was 49,775±16,071(range 25,248-142,345). The values of Good's coverage of all libraries were above 99%. The species accumulation curve showed that the estimated OTU richness already approached saturation at this sequencing depth, suggesting that a vast majority of diversity had been detected (Figure 1A). A Venn diagram showed that 541 of the total 698 OTUs were shared among the three groups, while 31 were unique for IgAN, and 16 were specific for MN (Figure 1B). No significant differences in community richness (estimated by chao and ACE indices) and diversity(measured by Shannon and Simpson indices) were observed between IgAN and the healthy control(Supplemental Table 3, Supplemental Fig. 1A, B, C, D).Similar trends for community richness and diversity were observed between IgAN and MN, consistent with the trends observed between MN and healthy control(Supplemental Table 3; Supplemental Fig. 1A, B, C, D).

Taxonomy-based comparisons of gut microbiota at the phylum and genus levels

At the phylum level, the gut microbiota of the three groups was dominated by Firmicutes, Bacteroidetes, Proteobacteria, and Actinobacteria, which on average accounted for up to 98% of the relative abundance (Figure 2A). Bacterial genera *Bacteroides*, *Faecalibacterium*, *Prevotella*, and *Lachnospiraceae_incertae_sedis*, each accounting for up to 5% of the sequences on average, were the

dominant populations (Figure 2B). The faecal microbial composition of all samples at the phylum and genus levels is shown in the Supplemental Figure 2A, B.

IgA Nephropathy versus Healthy Controls

Firmicutes was the most predominant phylum, contributing 47.5% and 50.7% of the gut microbiota in patients with IgAN and healthy controls, respectively. Compared to that in the healthy controls, Proteobacteria and Candidate_division_TM7were overrepresented (8.37% vs. 3.41% and 0.026% vs. 0.013%, respectively), while Fusobacteria and Synergistetes were significantly underrepresented in patients with IgAN (0.25% vs. 0.29% and 0.013% vs. 0.018%, respectively, all $P<0.05$, Figure 2C, Supplemental Table 4). At the genus level, we observed that *Escherichia-Shigella* and *Defluviitaleaceae_incertae_sedis* were enriched in IgAN(5.67% vs. 1.04% and 0.17% vs. 0.12%, respectively), while five genera, namely, *Roseburia, Lachnospiraceae*_unclassified, *Clostridium_sensu_stricto_1*, *Haemophilus*, and *Fusobacterium* were enriched in the healthy control(3.52% vs. 4.28%, 0.39% vs. 0.72%, 0.12% vs. 1.02%, 0.03% vs. 0.22%, and 0.25% vs. 0.29%, respectively, all $P<0.05$, Figure 2D, Supplemental Table 5).

Membranous Nephropathy versus Healthy Controls

Firmicutes was the dominant phylum in both MN and HC, contributing 47.2% and 50.7% of the gut microbiota, respectively. At the phylum level, the abundance of Proteobacteria increased (9.86% vs. 3.41%), whereas that of Synergistetes decreased in patients with MN compared to that in the healthy controls (0.008% vs. 0.018%, all $P<0.05$, Figure 2E, Supplemental Table 4). At the genus level, the abundance of five genera, namely, *Escherichia-Shigella, Streptococcus*, *Enterobacteriaceae*_unclassified, *Peptostreptococcaceae_incertae_sedis,* and *Enterococcus* increased(6.24% vs. 1.04%, 0.61% vs. 0.29%, 1.01% vs. 0.11%, 0.18% vs. 0.10%, and 0.045% vs. 0.007%), whereas the abundance of four genera, namely, *Lachnospira*, *Lachnospiraceae*_unclassified, *Clostridium_sensu_stricto_1*, and *Veillonella* decreased in patients with MN compared to that in the healthy controls (0.63% vs. 1.83%, 0.43% vs. 0.72%, 0.28% vs. 1.02%, and 0.28% vs. 0.42%, all $P<0.05$, Figure 2F, Supplemental Table 5).

IgA Nephropathy versus Membranous Nephropathy

Next, we investigated how microbial populations vary between disease cohorts, although no significant differences were observed at the phylum level between IgAN and MN. Compared to that in MN, the abundance of genera *Megasphaera* and *Bilophila* increased (1.23% vs. 0.17% and 0.23% vs. 0.09%), whereas those of *Veillonella, Klebsiella*, *Haemophilus, Enterococcus,* and *Streptococcus* decreased in patients with IgAN(0.25% vs. 0.28%, 0.33% vs. 0.91%, 0.03% vs. 0.43, 0.006% vs. 0.04%,and 0.17% vs. 1.01%, all $P<0.05$, Figure 2G,Supplemental Table 5).

Identification of Key OTUs

To identify key phylotypes distinguishing different groups, OTUs with a median relative abundance larger than 0.01% were analyzed using a Random Forest model. Compared to that in the healthy control, we

identified 15 OTUs specific for IgAN, among which six OTUs assigned to *Bifidobacterium*, *Paraprevotella*, *Parabacteroides*, *Roseburia*, and *Defluviitaleaceae_incertae_sedis* were enriched, while nine OTUs assigned to *Lachnospiraceae*_unclassified, *Haemophilus*, *Clostridium_sensu_stricto_1*, *Bacteroides*, *Ruminococcaceae_incertae_sedis*, *Megamonas*, *Faecalibacterium*, and *Roseburia* were depleted in IgAN. Furthermore, we identified 15 OTUs specific for MN, among which seven OTUs assigned to *Bacteroides*, *Escherichia-Shigella*, *Streptococcus*, and *Lachnospiraceae_incertae_sedis* were enriched, while eight OTUs assigned to *Bacteroides*, *Lachnospiraceae*_unclassified, *Clostridium_sensu_stricto_1*, *Lachnospira*, *Lachnospiraceae_incertae_sedis*, *Ruminococcaceae_incertae_sedis*, *Subdoligranulum*, and *Ruminococcus* were depleted in MN. Furthermore, we found 12 OTUs as key variables between patients with IgAN and MN, among which three OTUs assigned to *Flavonifractor*, *Veillonella* and *Ruminococcaceae_incertae_sedis* were enriched in IgAN, while nine OTUs assigned to *Veillonella*, *Haemophilus*, *Gemella*, *Lactobacillus*, *Bacteroides*, *Klebsiella*, *Actinomyces* and *Streptococcus* were enriched in MN(Figure 3A,B,C).

Differentiation of patients Based on Gut Microbiota Profiles

PCoA based on unweighted UniFrac distances revealed that the microbial composition of IgAN deviated from those of the healthy controls (P=0.007, Figure 4A). The patients with MN and healthy control samples also separated when subjected to PCoA (P=0.018, Figure 4B). Conversely, a symmetrical distribution was observed between IgAN and MN when subjected to PCoA based on unweighted UniFrac distances (P=0.633, Supplemental Figure 3). To identify the specific taxa between groups, we analyzed faecal microbiota using LEfSe. A cladogram presented the gut microbial structures and the major differences in taxa between patients with IgAN and healthy controls (Supplemental Figure 4A, B). We also compared the faecal microbiota to identify the specific taxa between patients with MN and healthy controls (Supplemental Figure 4C, D); results showed gut microbial dysbiosis in patients with IgAN and MN. Further, the cladogram of microbial structure obtained after comparison of the faecal microbiota between disease cohorts showed the maximum differences in taxa (Supplemental Figure 4E, F).

Spearman correlation test in patients with IgAN and MN

Pairwise comparisons of clinical factors were shown, with a color gradient denoting Spearman's correlation coefficients. The clinical factors were mainly focused on the risk factors for kidney prognosis. In IgAN group, significant positive correlation existed between the genera *Klebsiella* and *Enterobacteriaceae*_unclassified(ρ=0.82, Figure 5A). In addition, the genus *Prevotella* showed positive correlation, while *Klebsiella*, *Citrobacter*, and *Fusobacterium* showed negative correlations with serum albumin (ALB) level. Positive correlations existed between *Bilophila* and Crescents in the Oxford classification of IgAN (Figure 5A, Supplemental Table 6). Correspondingly, in the MN group, significant positive correlations existed in the genera: *Alistipes* and *Ruminococcaceae*_uncultured(ρ=0.82), *Anaerotruncus* and *Christensenellaceae*_uncultured(ρ=0.87), *Citrobacter* and *Enterobacteriaceae*_unclassified(ρ=0.81, Figure 5B). Negative correlation existed between *Escherichia-Shigella* and proteinuria, *Bacteroides* and *Klebsiella* showed positive correlation with the MN stage, while

Akkermansia showed negative correlation with IgG4 deposition in the subepithelia, as observed using immunofluorescence (Figure 5B, Supplemental Table 7).

Discussion

To our knowledge, our present study represents the characterization of the gut microbiota in patients with IgAN and MN. In our present study, we demonstrated patterns of gut microbiota dysbiosis in two most prevalent glomerulonephritis and identified taxa specific for patients and healthy controls. The results of this study are twofold. First, using differential abundance analyses, we identified that patients with IgAN and MN were characterized by altered composition of the stool microbiota. Second, we showed the dissimilitude of the microbial community between patients with IgAN and MN.

We observed numerous taxonomic differences between disease cohorts and healthy controls. Compared to that in the control, the ethanol-producing genus *Escherichia-Shigella*[23] was enriched, consistent with the previous study[21], whereas the butyrate-producing genera *Roseburia* and *Faecalibacterium*[24,25]were depleted in patients with IgAN. The opportunistic pathogens *Escherichia-Shigella* occur predominantly in patients with diabetic nephropathy [22]and Crohn's disease[2]. The increase in *Escherichia-Shigella* population may exacerbate gut leakiness by decreasing butyrate biosynthesis and increasing oxidative stress to penetrate the intestinal epithelial barrier[26].

Compared to that in the healthy controls, the genus *Roseburia* has been reported to be depleted in Crohn's disease[27]. Interestingly, patients with Crohn's disease on anti-TNFα antibody therapy showed increase in *Roseburia* abundance[28]. Underrepresentation of the genus *Faecalibacterium* has been implicated in several disorders, including inflammatory bowel disease(IBD)[29] and obesity[30]. *In vitro*, the culture supernatant of *Faecalibacterium* has been shown to inhibit nuclear factor-κB(NF-κB) activation, which is involved in the pathogenesis of IgAN[10]. As the major source of energy in the intestinal mucosa [31], butyrate plays an important role in maintaining gut health by exerting anti-inflammatory effects[24] and affects regulatory T (Treg) cells, which participate in the pathogenesis of IgAN[32]. Hence, *Roseburia* and *Faecalibacterium* were reported to be potential markers of gut health [24,25].The reduction in butyrate-producing genera may promote intestinal mucosal destruction[33], which plays a critical step in the pathogenesis of IgAN[10]. Increasing evidence from human studies suggests that *Roseburia* and *Faecalibacterium* are potential probiotic candidates for the treatment of chronic gut inflammation[34].

Interestingly, *Bifidobacterium* abundance was higher in patients with IgAN than in healthy controls. As probiotic microorganisms, members of the genus *Bifidobacterium* are beneficial for health as they affect immune regulation[35], inhibit pathogens[36], and degrade diet-derived carbohydrates[37]. Out of more than 50 species assigned to *Bifidobacterium*, only 10 are found in humans. However, a previous study demonstrated the invasive potential of *Bifidobacterium* in immune compromised host[38]. Another study identified higher abundance of *Bifidobacterium* in patients with ulcerative colitis[27] than in healthy

controls. Thus, we propose that some species may be disease-specific and further investigation regarding their effect on gut homeostasis is required.

Investigation of the relationships between clinical parameters and microbial taxa in the IgAN group revealed that *Prevotella* was associated with higher level of ALB, while *Klebsiella*, *Citrobacter,* and *Fusobacterium* were associated with lower level of ALB. *Prevotella* has previously been reported to be associated with improved glucose metabolism and insulin sensitivity[39], while *Klebsiella* correlated with the invasion of epithelial cells[25].

Compared to that in the healthy controls, the abundance of *Escherichia-Shigella*, *Bacteroides*, *Actinomyces,* and *Streptococcus* increased, while those of *Lachnospira* and *Roseburia* decreased in patients with MN. *Escherichia-Shigella* and *Bacteroides* have been reported to produce lipopolysaccharide (LPS)[40], which initiates various pathophysiological cascades[41]. High levels of LPS activate the NF-κB pathway and lead to the production of pro-inflammatory cytokines(TNF-α, IL-6, and IL-1)[41]. In agreement with this observation, higher abundance of *Escherichia-Shigella* and *Bacteroides* increases the circulating levels of pro-inflammatory cytokines such as TNF-α and IL-6, and genetic polymorphisms in these cytokines are associated with the onset/occurrence of MN[42,43]. *Actinomyces* has been identified to be abundant in patients with rheumatoid arthritis[44] and ulcerative colitis[45]. Members of the genus *Streptococcus* has recently been associated with numerous immune-mediated inflammatory diseases [28,46]. Furthermore, the presence of *Streptococcus* may be a predictive marker for the future recurrence of Crohn's disease[2]. Butyrate-producing *Lachnospira* and *Roseburia* are potential markers of health. *Akkermansia* displayed negative correlations with IgG4 deposition in the subepithelia. *Akkermansia muciniphila*, which produces the protective mucous lining of the intestine[47], is associated with health and the absence of autoimmune diseases[48].

Genetic susceptibilities and immune dysregulation are believed to be involved in the pathogenesis of IgAN and MN. Numerous environmental factors are known to affect the gut microbial community. Thus, it is not surprising that the abundance of certain taxa differs in the gut microbiota of patients and healthy controls. It is noteworthy that compared to that in healthy controls, taxa such as *Ruminococcaceae_incertae_sedis* were more abundant in IgAN and less abundant in MN. *Ruminococcaceae* was enriched in patients with hepatic encephalopathy[49], although evidence linking *Ruminococcaceae_incertae_sedis* to the disease is lacking. Therefore, it has been hypothesized that the varying abundance of certain taxa may influence autoimmune response and distant organs. Further studies are required to confirm the possible roles these microorganisms in the etiology of glomerulopathy. We identified certain genera (and OTUs) to be uniquely represented in patients compared to in healthy controls. Furthermore, we also identified certain taxa that were significantly different between patients with IgAN and MN. Considering the different pathological patterns of glomerulopathy, it is not surprising that we detected these differences.

Compared to that in the healthy controls, we observed alterations in the gut microbial community in the treatment-naïve IgAN and MN patients, which indicated that certain bacterial candidates may be implicated in disease pathogenesis and can be used as specific biomarkers in the patient cohort.

Despite the promising results, our study has certain limitations. First, we tested a relatively small sample size at the moderate pathological stage; a larger cohort that includes patients at different pathological stages will be necessary to comprehensively study the role of the gut microbiota and further validate these findings. Similarly, sufficient sample size will be required for comparisons across different disease states (active and inactive) and treatments. Data regarding the role of an active immune response and immunomodulating therapies on the gut microbiota are also limited. Second, although age, gender, and BMI were matched in our study, certain confounding effects such as dietary factors, should also be considered. However, the participants in our study were from northwest of China, and the lifestyle factors were similar. Third, we analyzed faecal microbiota, which cannot fully reflect the profiles of mucosal microbiota.

The results of our study demonstrated that alteration of gut microbiota is associated with developments of IgAN and MN, evidenced by the changes in various taxonomic levels. The specific microbes may be potential diagnostic biomarkers and therapeutic targets for IgAN and MN. Potential therapeutic strategies for IgAN and MN that target the gut microbiota by faecal microbiota transplantation are already being investigated.

Conclusion

In summary, this study presents a comprehensive analysis of the gut microbiota composition in patients with IgAN and MN. We showed that the composition of the gut microbiota differs significantly in patients with IgAN and MN compared to that in the healthy controls. Further investigations are warranted to establish the causality in disease pathogenesis and diagnostic potential.

List Of Abbreviations

BMI, body mass index; BP, blood pressure; WBC, white blood cell count; Hb, hemoglobin; Plt, platelet count; TP, total protein; ALB, albumin; S-Cre, serum creatinine; eGFR, glomerular filtration rate; PLA2R, phospholipase A2 receptor.

Declarations

Ethics approval and consent to participate

The protocol of the study was approved by the Ethics Committee of Xijing Hospital of The Fourth Military Medical University. All the subjects provided their written consent for participation in this study. The procedures were followed in accordance with the Declaration of Helsinki.

Consent for publication

Not applicable.

Availabilty of data and material

The raw read data of all the samples have been deposited in the European Bioinformatics Institute European Nucleotide Archive database under the accession number: PRJNA574226.

Competing interests

The authors declare that they have no competing interests.

Funding

This study was sponsored by a grant from the discipline boosting program of the Xijing Hospital of the Fourth Military Medical University(XJZT18Z15). Key research and development plan of Shaanxi province, China (No. 2017ZDXM-SF-045).

Author contribution

SS and MB designed and supervised the project. RD and JZ collected samples. DW performed pathological diagnosis. RD contributed to data collection. RD and JZ performed bioinformatics and statistical analysis, and interpreted data. RD drafted the manuscript. SS and MB revised the manuscript for important content. Each author contributed important content, accepts personal accountability for the author's own contributions, and agrees to ensure that questions pertaining to the accuracy or integrity of any portion of the work are appropriately investigated and resolved.

Acknowledgments

We thank Dr Hongyan Ren(Shanghai Mobiomed Technology Co., Ltd., China) for Miseq sequencing. We also thank the clinical doctors from the Xijing Hospital, the Fourth Military Medical University. We also thank the volunteers who enrolled for the study.

References

1. Meijers B, Evenepoel P, Anders HJ. Intestinal microbiome and fitness in kidney disease. Sep 2019;15(9):531-545.
2. Pascal V, Pozuelo M, Borruel N, et al. A microbial signature for Crohn's disease. *Gut.* May 2017;66(5):813-822.
3. Morgan XC, Tickle TL, Sokol H, et al. Dysfunction of the intestinal microbiome in inflammatory bowel disease and treatment. *Genome biology.* Apr 16 2012;13(9):R79.

4. Hevia A, Milani C, Lopez P, et al. Intestinal dysbiosis associated with systemic lupus erythematosus. *mBio.* Sep 30 2014;5(5):e01548-01514.
5. Wen C, Zheng Z, Shao T, et al. Quantitative metagenomics reveals unique gut microbiome biomarkers in ankylosing spondylitis. Jul 27 2017;18(1):142.
6. Zhang X, Zhang D, Jia H. The oral and gut microbiomes are perturbed in rheumatoid arthritis and partly normalized after treatment. Aug 2015;21(8):895-905.
7. Xu X, Wang G, Chen N, et al. Long-Term Exposure to Air Pollution and Increased Risk of Membranous Nephropathy in China. *Journal of the American Society of Nephrology : JASN.* Dec 2016;27(12):3739-3746.
8. Zhang YM, Zhang H. Insights into the Role of Mucosal Immunity in IgA Nephropathy. *Clinical journal of the American Society of Nephrology : CJASN.* Oct 8 2018;13(10):1584-1586.
9. Magistroni R, D'Agati VD, Appel GB, Kiryluk K. New developments in the genetics, pathogenesis, and therapy of IgA nephropathy. *Kidney international.* Nov 2015;88(5):974-989.
10. Kiryluk K, Li Y. Discovery of new risk loci for IgA nephropathy implicates genes involved in immunity against intestinal pathogens. Nov 2014;46(11):1187-1196.
11. Coppo R. The Gut-Renal Connection in IgA Nephropathy. *Seminars in nephrology.* Sep 2018;38(5):504-512.
12. Couser WG. Primary Membranous Nephropathy. *Clinical journal of the American Society of Nephrology : CJASN.* Jun 7 2017;12(6):983-997.
13. Beck LH, Jr., Bonegio RG, Lambeau G, et al. M-type phospholipase A2 receptor as target antigen in idiopathic membranous nephropathy. *The New England journal of medicine.* Jul 2 2009;361(1):11-21.
14. Godel M, Grahammer F, Huber TB. Thrombospondin type-1 domain-containing 7A in idiopathic membranous nephropathy. *The New England journal of medicine.* Mar 12 2015;372(11):1073.
15. De Vriese AS, Glassock RJ, Nath KA, Sethi S, Fervenza FC. A Proposal for a Serology-Based Approach to Membranous Nephropathy. *Journal of the American Society of Nephrology : JASN.* Feb 2017;28(2):421-430.
16. Debiec H, Lefeu F, Kemper MJ, et al. Early-childhood membranous nephropathy due to cationic bovine serum albumin. *The New England journal of medicine.* Jun 2 2011;364(22):2101-2110.
17. Lee N, Kim WU. Microbiota in T-cell homeostasis and inflammatory diseases. *Experimental & molecular medicine.* May 26 2017;49(5):e340.
18. Ronco P, Debiec H. Pathophysiological advances in membranous nephropathy: time for a shift in patient's care. *Lancet (London, England).* May 16 2015;385(9981):1983-1992.
19. Cesta MF. Normal structure, function, and histology of mucosa-associated lymphoid tissue. *Toxicologic pathology.* 2006;34(5):599-608.
20. Fresquet M, Jowitt TA, Gummadova J, et al. Identification of a major epitope recognized by PLA2R autoantibodies in primary membranous nephropathy. *Journal of the American Society of Nephrology*

: JASN. Feb 2015;26(2):302-313.

21. De Angelis M, Montemurno E, Piccolo M, et al. Microbiota and metabolome associated with immunoglobulin A nephropathy (IgAN). *PloS one.* 2014;9(6):e99006.
22. Tao S, Li L, Li L, et al. Understanding the gut-kidney axis among biopsy-proven diabetic nephropathy, type 2 diabetes mellitus and healthy controls: an analysis of the gut microbiota composition. May 2019;56(5):581-592.
23. Clark DP. The fermentation pathways of Escherichia coli. *FEMS microbiology reviews.* Sep 1989;5(3):223-234.
24. Tamanai-Shacoori Z, Smida I, Bousarghin L, et al. Roseburia spp.: a marker of health? *Future microbiology.* Feb 2017;12:157-170.
25. Tang R, Wei Y, Li Y, et al. Gut microbial profile is altered in primary biliary cholangitis and partially restored after UDCA therapy. *Gut.* Mar 2018;67(3):534-541.
26. Croxen MA, Law RJ, Scholz R, Keeney KM, Wlodarska M, Finlay BB. Recent advances in understanding enteric pathogenic Escherichia coli. *Clinical microbiology reviews.* Oct 2013;26(4):822-880.
27. Forbes JD, Chen CY, Knox NC, et al. A comparative study of the gut microbiota in immune-mediated inflammatory diseases-does a common dysbiosis exist? *Microbiome.* Dec 13 2018;6(1):221.
28. Lewis JD, Chen EZ, Baldassano RN, et al. Inflammation, Antibiotics, and Diet as Environmental Stressors of the Gut Microbiome in Pediatric Crohn's Disease. *Cell host & microbe.* Aug 9 2017;22(2):247.
29. Sokol H, Seksik P, Furet JP, et al. Low counts of Faecalibacterium prausnitzii in colitis microbiota. *Inflammatory bowel diseases.* Aug 2009;15(8):1183-1189.
30. Turnbaugh PJ, Backhed F, Fulton L, Gordon JI. Diet-induced obesity is linked to marked but reversible alterations in the mouse distal gut microbiome. *Cell host & microbe.* Apr 17 2008;3(4):213-223.
31. Louis P, Flint HJ. Diversity, metabolism and microbial ecology of butyrate-producing bacteria from the human large intestine. *FEMS microbiology letters.* May 2009;294(1):1-8.
32. Ruszkowski J, Lisowska KA, Pindel M, Heleniak Z, Debska-Slizien A, Witkowski JM. T cells in IgA nephropathy: role in pathogenesis, clinical significance and potential therapeutic target. *Clinical and experimental nephrology.* Mar 2019;23(3):291-303.
33. Ren Z, Li A, Jiang J, et al. Gut microbiome analysis as a tool towards targeted non-invasive biomarkers for early hepatocellular carcinoma. *Gut.* Jun 2019;68(6):1014-1023.
34. Sanders ME, Merenstein DJ, Reid G. Author Correction: Probiotics and prebiotics in intestinal health and disease: from biology to the clinic. Aug 9 2019.
35. Round JL, Mazmanian SK. The gut microbiota shapes intestinal immune responses during health and disease. *Nature reviews. Immunology.* May 2009;9(5):313-323.
36. Serafini F, Strati F, Ruas-Madiedo P, et al. Evaluation of adhesion properties and antibacterial activities of the infant gut commensal Bifidobacterium bifidum PRL2010. *Anaerobe.* Jun 2013;21:9-

17.
37. Pokusaeva K, Fitzgerald GF, van Sinderen D. Carbohydrate metabolism in Bifidobacteria. *Genes & nutrition.* Aug 2011;6(3):285-306.
38. Esaiassen E, Hjerde E, Cavanagh JP, Simonsen GS, Klingenberg C. Bifidobacterium Bacteremia: Clinical Characteristics and a Genomic Approach To Assess Pathogenicity. *Journal of clinical microbiology.* Jul 2017;55(7):2234-2248.
39. De Vadder F, Kovatcheva-Datchary P, Zitoun C, Duchampt A, Backhed F, Mithieux G. Microbiota-Produced Succinate Improves Glucose Homeostasis via Intestinal Gluconeogenesis. *Cell metabolism.* Jul 12 2016;24(1):151-157.
40. Wexler HM. Bacteroides: the good, the bad, and the nitty-gritty. *Clinical microbiology reviews.* Oct 2007;20(4):593-621.
41. Darnaud M, Faivre J, Moniaux N. Targeting gut flora to prevent progression of hepatocellular carcinoma. *Journal of hepatology.* Feb 2013;58(2):385-387.
42. Thibaudin D, Thibaudin L, Berthoux P, et al. TNFA2 and d2 alleles of the tumor necrosis factor alpha gene polymorphism are associated with onset/occurrence of idiopathic membranous nephropathy. *Kidney international.* Mar 2007;71(5):431-437.
43. Chen SY, Chen CH, Huang YC, Chuang HM, Lo MM, Tsai FJ. Effect of IL-6 C-572G polymorphism on idiopathic membranous nephropathy risk in a Han Chinese population. *Renal failure.* 2010;32(10):1172-1176.
44. Thota VR, Dacha S, Natarajan A, Nerad J. Eggerthella lenta bacteremia in a Crohn's disease patient after ileocecal resection. *Future microbiology.* May 2011;6(5):595-597.
45. Forbes JD, Van Domselaar G, Bernstein CN. Microbiome Survey of the Inflamed and Noninflamed Gut at Different Compartments Within the Gastrointestinal Tract of Inflammatory Bowel Disease Patients. *Inflammatory bowel diseases.* Apr 2016;22(4):817-825.
46. Chen J, Chia N, Kalari KR, et al. Multiple sclerosis patients have a distinct gut microbiota compared to healthy controls. *Scientific reports.* Jun 27 2016;6:28484.
47. Berry D, Stecher B, Schintlmeister A, et al. Host-compound foraging by intestinal microbiota revealed by single-cell stable isotope probing. *Proceedings of the National Academy of Sciences of the United States of America.* Mar 19 2013;110(12):4720-4725.
48. Routy B, Gopalakrishnan V, Daillere R, Zitvogel L, Wargo JA, Kroemer G. The gut microbiota influences anticancer immunosurveillance and general health. *Nature reviews. Clinical oncology.* Jun 2018;15(6):382-396.
49. Bajaj JS. The role of microbiota in hepatic encephalopathy. *Gut microbes.* May-Jun 2014;5(3):397-403.

Tables

Table 1 Baseline characteristics of study individuals.

Clinical indexes	IgAN(n=44)	MN(n=40)	HC (n=30)	*P*
Age, y	34.89±10.74	43.13±13.81	38.60±12.80	0.012
Male sex	20(45.5%)	26(65.0%)	14(46.7%)	0.150
BMI, kg/m^2	22.95±3.17	23.76±3.15	22.78±2.32	0.310
Hypertension	11(25.0%)	12(30.0%)	-	0.005
Systolic BP, mmHg	126.05±18.31	126.98±18.78	112.33±9.98	0.001
Diastolic BP, mmHg	78.86±15.37	76.38±12.42	71.77±8.21	0.067
WBC, $10^9/L$	6.71±1.71	6.55±1.37	5.59±1.22	0.004
Hb, g/L	136.75±22.77	143.25±20.73	146.53±16.38	0.113
PLT, $10^9/L$	249.02±96.07	250.0±64.60	212.30±57.49	0.079
TP, g/L	69.40±6.68[a]	51.45±8.24[b]	74.45±3.88	<0.001
ALB, g/L	42.10±5.32[c]	26.90±6.77[d]	48.21±3.35	<0.001
S-Cre, umol/L	102.04±32.33[e]	79.73±20.66	83.85±16.99	<0.001
eGFR, $mL/min/1.73m^2$	73.30±23.94	98.15±23.24	85.04±18.24	<0.001
Hematuria	44(100%)	31(77.5%)	-	-
Nephrotic syndrome	2(4.5%)	33(82.5%)	-	-
Proteinuria, mg/24h	776[384-1372]	3623[2000-6493]	-	-
Anti-PLA2R antibody positivity	0(0%)	29(72.5%)	-	-

Note: Continuous data presented as mean±standard deviation or median [interquartile range]; categorical variables were presented as number (%). One-way ANOVA was used to evaluate continuous variables and Chi-square test was used to compare categorical variables among the three groups. Two-tailed t test was used to evaluate continuous variables and Chi-square test was used to compare categorical variables between the two groups.

Abbreviations: BMI, body mass index; BP, blood pressure; WBC, white blood cell count; Hb, hemoglobin; Plt, platelet count; TP, total protein; ALB, albumin; S-Cre, serum creatinine;

eGFR, glomerular filtration rate; PLA2R, phospholipase A2 receptor.

[a,c,e] *P* values are from t test between IgAN group and HC group, [b,d] *P* values are from t test between MN group and HC group. They are statistical different.

Table 2 Pathological features of the patients with IgAN and MN.

Pathological features	IgAN(N=44)	Pathological features	MN(N=40)
Oxford classification		Glomerular lesion of MN	
Mesangial hypercellularity (M0/M1)	22/22(50%/50%)	Stage Ⅰ,n(%)	2(5%)
Segmental glomerulosclerosis (S0/S1)	10/34(22.7%/77.3%)	Stage Ⅱ,n(%)	35(87.5%)
Endocapillary hypercellularity (E0/E1)	41/3(93.2%/6.8%)	Stage Ⅲ,n(%)	3(7.5%)
Tubular atrophy/interstitial fibrosis (T0/T1/T2)	34/8/2(77.3%/18.2%/4.5%)	Stage Ⅳ,n(%)	0(0%)
Crescents(C0/C1/C2)	37/7/0(84.1%/15.9%/0%)		

Note: Categorical variables were presented as number (%).

Abbreviations: M, mesangial hypercellularity (M0, <50% of glomeruli show mesangial hypercellularity; M1, >50% of glomeruli show mesangial hypercellularity); S, segmental glomerulosclerosis (S0, absent; S1, present in any glomeruli); E, endocapillary hypercellularity (E0, no endocapillary hypercellularity; E1, any glomeruli show

endocapillary hypercellularity); T, tubular atrophy/interstitial fibrosis (T0, 0%-25% of cortical area; T1, 26%-50% of cortical area; T2, >50% of cortical area); C, crescents (C0: absent; C1, 0%-25% of glomeruli; C2, ≥25% of glomeruli).

Figures

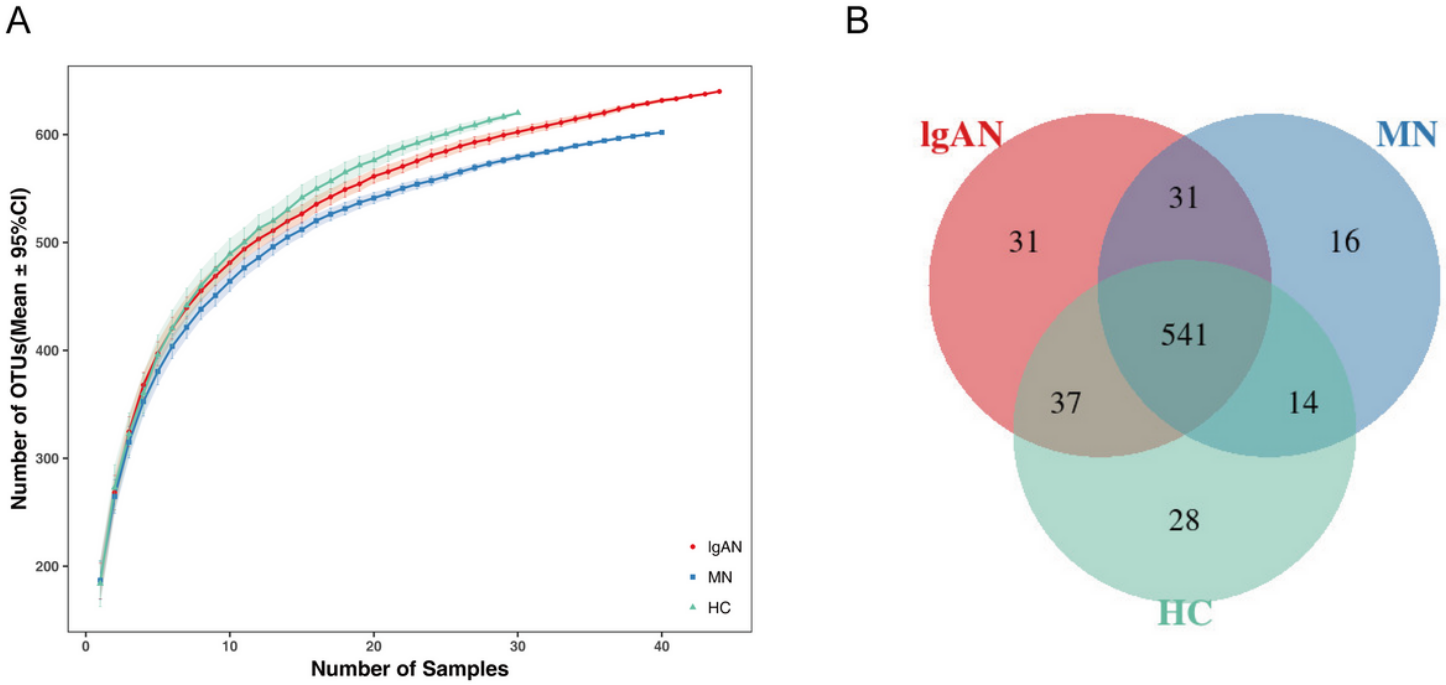

Figure 1

Species accumulation curves and Venn diagram of IgAN, MN and HC groups. (A) Species accumulation curves between number of samples and estimated richness. The estimated OTUs richness were close to saturation in each group. (B) A Venn diagram displaying the overlaps between groups that 541 of the total 698 OTUs were shared among the three groups, while 31 were unique for IgAN, 16 were specific for MN. IgAN, immunoglobulin A nephropathy; MN, membranous nephropathy; HC, healthy controls.

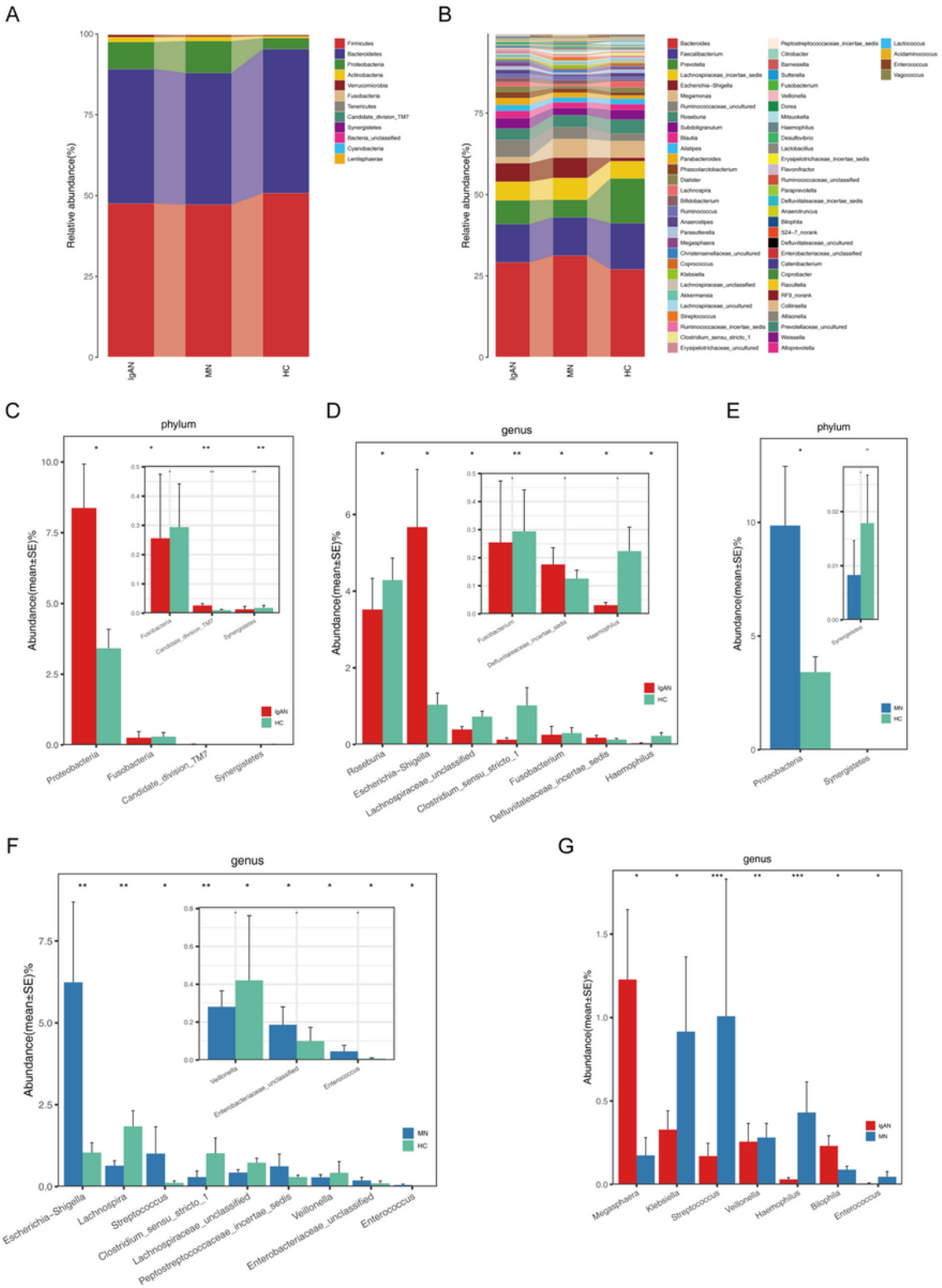

Figure 2

Phylogenetic profiles of gut microbes among patients with IgAN (n=44), patients with MN (n=40) and HC(n=30). Composition of faecal microbiota at the phylum level (A) and genus level (B) among the three groups. The different microbial community at the phylum level (C) and genus level (D) in IgAN patients versus HC. The different microbial community at the phylum level (E) and genus level (F) in MN patients versus HC. The different microbial community at the genus level (G) in IgAN patients versus MN patients.

*P<0.05, **P<0.01. IgAN, immunoglobulin A nedphropathy; MN, membranous nephropathy; HC, healthy controls.

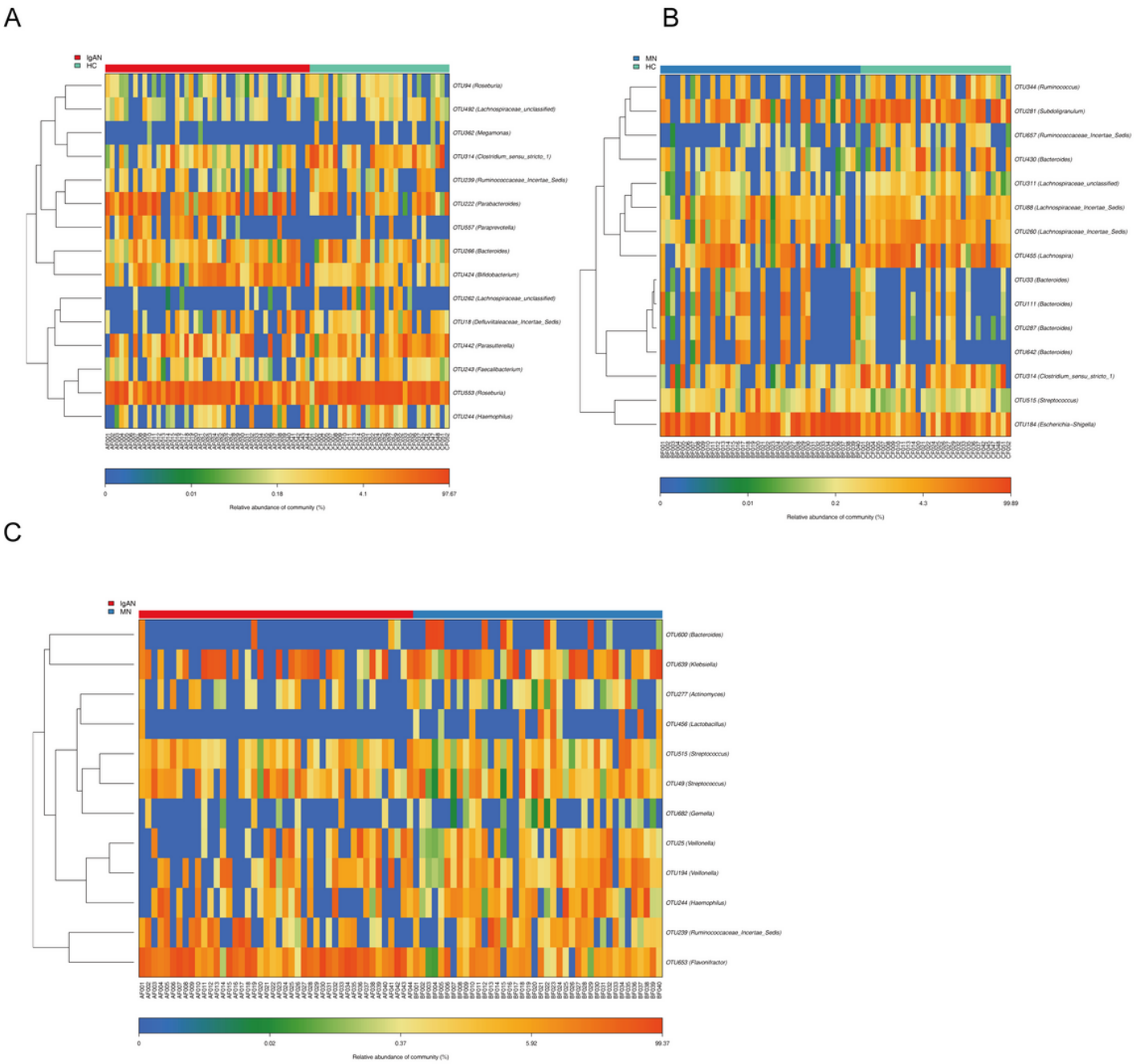

Figure 3

Identification of key Operational Taxonomy Units (OTUs) phylotypes between groups. (A) Abundance distribution of the 15 OTUs identified as key phylotypes for IgAN: six OTUs were enriched (orange font), while nine OTUs were decreased (blue font). (B) Abundance distribution of the 15 OTUs identified as key phylotypes for MN: seven OTUs were enriched (orange font), while eight OTUs were decreased (blue font). (C) Abundance distribution of the 12 OTUs identified as key variables between patients of IgAN and MN: three OTUs were increased in IgAN(orange font), 9 OTUs were increased in MN(orange font).

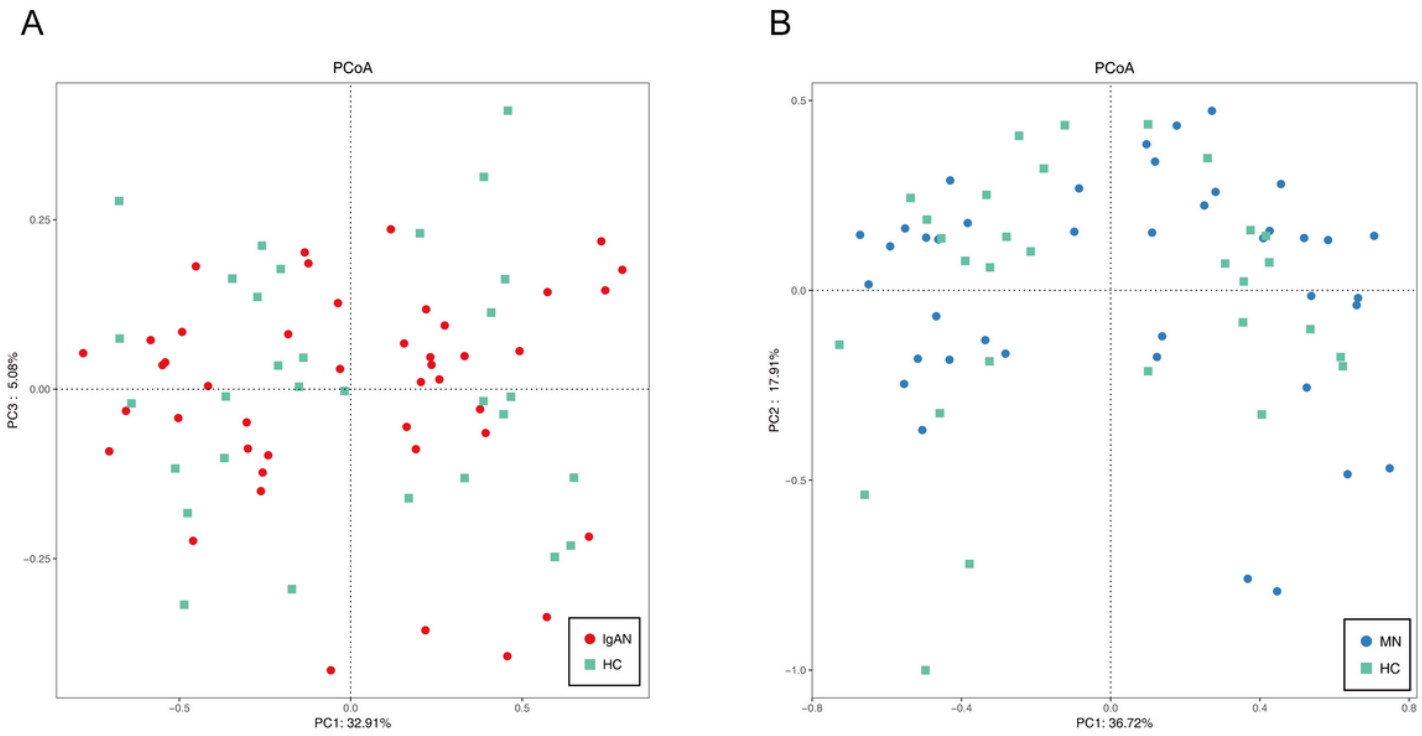

Figure 4

PCoA on the samples based on unweighted UniFrac distances. (A) PCoA of IgAN and HC. (B) PCoA of MN and HC. PCoA, principal coordinates analysis.

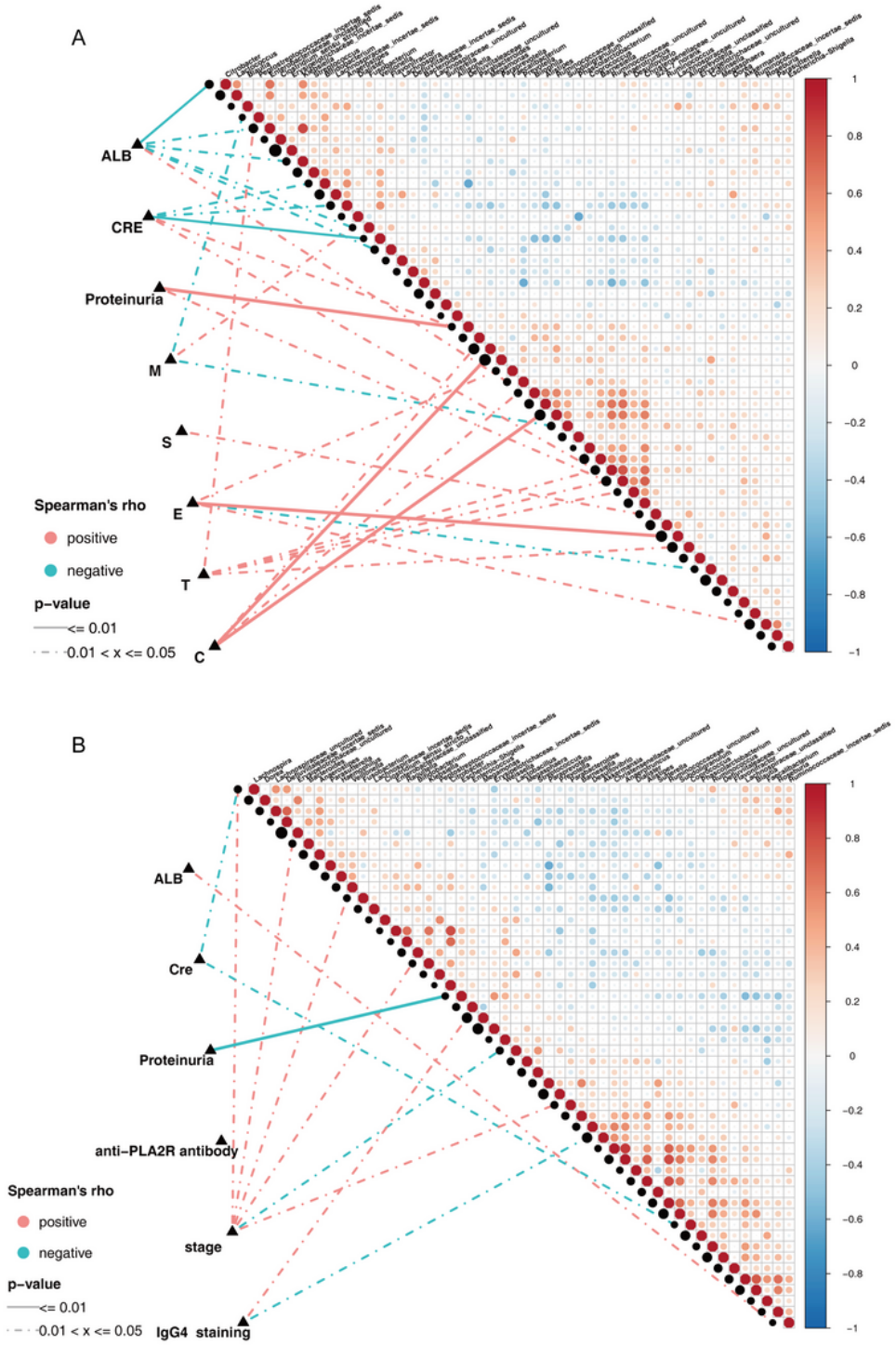

Figure 5

Spearman correlations in patients with IgAN and MN. (A) The oblique triangle heatmap indicated a taxon-taxon correlation in IgAN patients, the red circle represented positive correlation, the blue circle represented negative correlation. The correlation network indicated a correlation between faecal microbiota and clinical parameters in IgAN patients, the line of solid and dotted indicated strong and weak correlations respectively. (B) The oblique triangle heatmap indicated a taxon-taxon correlation in

MN patients, the red circle represented positive correlation, the blue circle represented negative correlation. The correlation network indicated a correlation between faecal microbiota and clinical parameters in MN patients, the line of solid and dotted indicated strong and weak correlations respectively.

Supplementary Files

This is a list of supplementary files associated with this preprint. Click to download.

- TableS3.docx
- Fig.S2.tif
- Fig.S3.tif
- SupplementalMaterial.docx
- Fig.S1.tif
- Fig.S4.tif
- TableS5.xlsx
- TableS6.xlsx
- TableS7.xlsx
- TableS1.xlsx
- TableS4.xlsx
- TableS2.xlsx